Development of High Strength Cold-rolled Steel-sheets with Excellent Phosphatability

Dr. Masahiro NOMURA; Materials Research Laboratory, Technical Development Group
Ikuro HASHIMOTO; Kobelco Research Institute, Inc.
Manabu KAMURA; Pro-Tec Coating Co. Quality Assurance
Shinji KOZUMA, Yoshinobu OMIYA; Research & Development Laboratory, Kakogawa Works, Iron & Steel Sector

High strength steel-sheets have become critically important in recent years in response to the growing demand for weight reduction and improved safety characteristics in automobile bodies. The conventional approach of strengthening steel has been to increase Si and Mn concentrations. However, these alloying elements have a significant negative influence on the resultant steel's phosphatability. In this study, oxides were analyzed on the surfaces of steels containing Si and Mn to clarify their effect on phosphatability. Attempts have been made to fabricate high strength steel-sheets with excellent phosphatability by controlling these surface oxides.

Introduction

Automotive industries are now working actively on environmental issues including global warming. Automotive weight reduction to decrease fuel consumption is regarded as a key to resolving the issue. Meanwhile, safety measures have been enhanced to protect occupants during collisions. To resolve these two issues, the materials for automobiles were made stronger. This is because the higher strength allows structural members to reduce their weights by decreasing the wall thicknesses, while retaining or even increasing the strength as structural members. High-strength, cold-rolled steel-sheets, among others, are required to have not only strength, but also elongation and ductility, since they are press-formed into various automotive parts such as body-frame members. To meet these requirements, various high-strength, high-elongation steels have been developed which include dual-phase (DP) steel and transformation-induced-plasticity (TRIP) steel[1)-4)].

Basic alloying elements, such as Si and Mn, are indispensable in achieving high-strength along with high-elongation. As the required strength becomes higher, the amounts of these elements added to steel are increased compared to conventional steel with relatively low strength. Meanwhile, these elements have been known to be easily-oxidizable, form oxides on the surfaces of steel-sheets[5)-9)] and significantly affect phosphatability[10), 11)].

With this background, the present study analyzed the effect of Si and Mn content on the oxide formed on steel-sheet surfaces. Also analyzed was the relation between the surface oxide conditions and phosphatability. In this study, steel-sheets with relatively high Si and Mn content were experimentally manufactured based on the results of the analyses. The steel-sheets have been found to exhibit good phosphatability along with high strength, elongation and other properties[12)]. This papar also includes the evaluation of the properties of the steel-sheets.

1. Experimental method

1.1 Analyses of oxides formed on steel-sheet surfaces

Phosphatability is significantly affected by the oxides on steel-sheet surfaces, as described previously. To clarify the distributions of oxides on the outermost surface of a steel-sheet, element mapping was first carried out using Auger electron spectroscopy (AES). The steel-sheets in **Table 1** were cut into 10 mm x 10 mm samples, of which surfaces were subjected to AES analysis[13)] to clarify the types and distributions of oxides formed on them. Following the AES analysis, cross-sectional transmission electron microscopy (TEM) was conducted to measure the oxide thickness and analyze the depth-distribution of the oxides. Concurrently, extraction replicas of the steel-sheet surfaces were prepared to analyze the oxides existing on the outermost surface layer. The replicas were prepared to avoid the effect from the matrix iron. The replicas were also analyzed by TEM to identify the types of oxides. The identifications were performed by elemental analyses using energy dispersive X-ray spectroscopy (EDX) equipped with TEM, and / or, by analyzing the diffraction spots obtained from the oxides.

Table 1 Chemical composition of analyzed steels (mass%)

Steel	C	Si	Mn	P	S
No.1	0.17	1.35	2.0	0.015	0.001
No.2	0.11	0.70	1.9	0.005	0.001

1.2 Evaluation of phosphatability

Phosphatability was evaluated on samples containing about 0 to 1.4 % Si and 0.2 to 2.5 % Mn. The samples

were phosphate-treated using commercially available phosphate-treatment solution (Palbond L3020 from Nihon Parkerizing Co.,Ltd). The treated surfaces were observed by scanning electron microscopy (SEM) to assess how phosphatability was affected by the crystalline conditions of zinc phosphate and especially by defects in the zinc phosphate coatings. Prior to the phosphate-treatment, types of oxides were identified by X-ray photoelectron spectroscopy (XPS) on the surfaces of the samples. Thus, the analyses were carried out systematically to clarify the relations among the Si and/or Mn content, phosphatability and surface oxides.

1.3 Prototype production of steel-sheets having excellent phosphatability

Based on the analytical results, two prototype steel-sheets, A and B, were produced, each of which is expected to have an excellent phosphatability and high strength/elongation balance. **Table 2** summarizes their chemical compositions. The prototype steel-sheets were annealed at 850ºC through a continuous annealing line. After the annealing, the steel-sheets A and B were cooled to 560ºC and 450ºC respectively, then quenched into water and were subjected to over-aging treatment at 200ºC.

As described in section 1.2, phosphatability was evaluated by SEM observations of phosphate-treated samples. Further, the samples were evaluated for their adhesion of coatings. Each phosphate-treated and painted sample was crosscut and submerged in a 5% NaCl solution for 240 hrs. Creep width was measured on each sample for the evaluation of its coating adhesion. The strength and elongation were measured using JIS#5 tensile test pieces taken from each of the prototype steel-sheets.

Table 2 Chemical composition of trial steels (mass%)

Steel	C	Si	Mn	P	S	Mo
A	0.08	0.7	2.4	0.010	0.001	0.20
B	0.08	1.0	3.0	0.010	0.001	—

2. Results and discussions

2.1 Analysis of oxides formed on the steel-sheet surfaces

Fig. 1 is a result of AES mapping showing the distributions of Fe and Si on the steel-sheets (steel-sheet #1 and #2). The steel-sheet #2 exhibits a homogenous elemental distribution, while the steel-sheet #1 indicates a contrasting distribution of Si. A sample taken from the steel-sheet #1 was phosphate-treated for a short period of 10 second. Immediately after the treatment, the zinc phosphate crystals formed on the surface were removed by hydrochloric acid. The relation was investigated between the contrasting distribution of Si and the region uncoated by zinc phosphate, and the result is shown in **Fig. 2**. It should be noted that the regions surrounded by red lines in Fig. 2 are the same region uncoated with zinc phosphate crystals, comparing the same region before and after the acid removal. The result clarifies that the uncoated region fits with the Si concentrated region measured by the AES mapping. Therefore, the distribution of Si on the steel-sheet surface is considered to significantly affect the adhesion of zinc phosphate, or phosphatability.

To clarify the thickness of the surface oxides and their distribution in the depth direction, each sample was subjected to cross-sectional TEM observations as shown in **Fig. 3**. The steel-sheet #1 exhibits a layer of about 50 nm. The EDX analysis of the layer detected O, Si, Fe and Cu. Since Cu is not an alloying element of the steel, the element is considered to have come from the TEM sample holder and not to be a

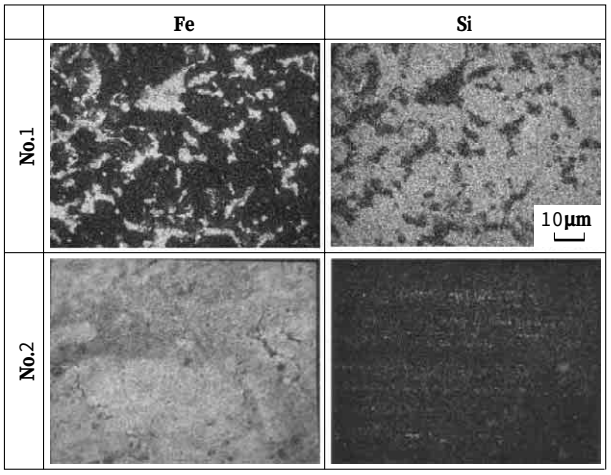

Fig. 1 Distribution of elements on steel surface before phosphate coating

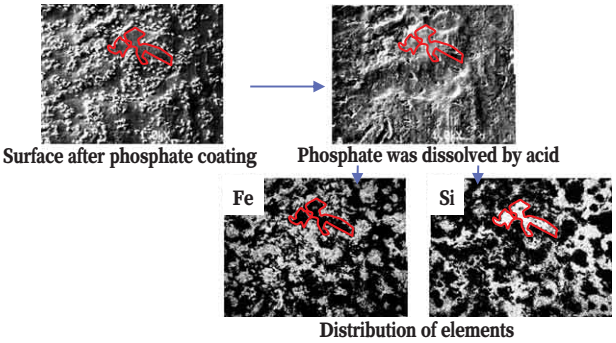

Fig. 2 Relationship between uncoated region and Si distribution

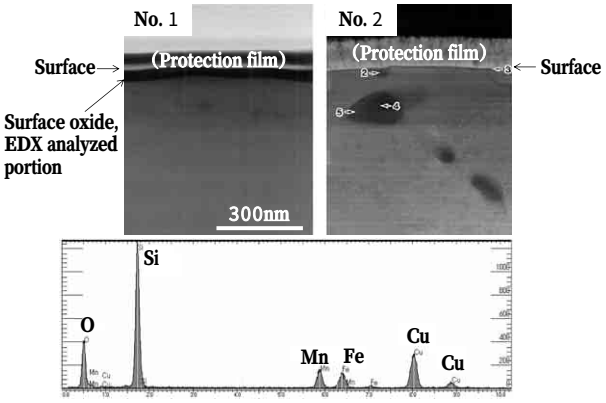

Fig. 3 Cross-sectional TEM image around steel surface

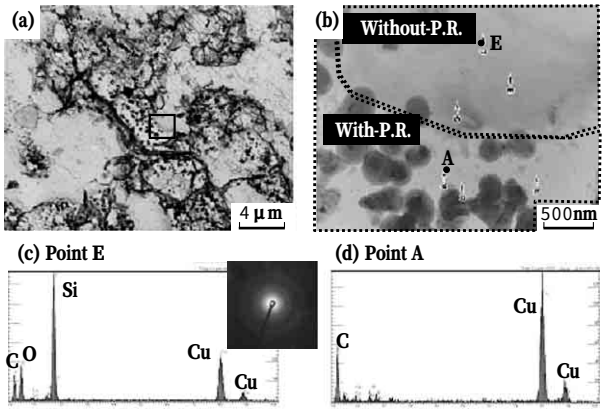

Fig. 4 TEM observation of extraction replica from steel surface
Two kinds of regions, (without/with particles) were observed

constituent of the layer. In addition, Fe possibly is originated from the matrix iron beneath the layer. Thus the layer is considered to be an oxide mainly consisting of Si, since the EDX profile shows a high intensity peak for Si and a clear peak of O.

On the other hand, the steel-sheet #2 exhibits particles which are considered to be granular oxides existing inside the iron matrix. Almost no oxide was observed on its surface. The cross sectional observation on the steel-sheet #2 shown in Fig. 3 agrees well with the observation shown in Fig. 1, illustrating that the outer most layer of the steel-sheet #2 is predominantly iron.

In order to analyze the above observed oxides in more detail, extraction replicas of the surface oxides were prepared and subjected to TEM observations. **Fig. 4** (a) and (b) show the TEM micrographs of an extraction replica prepared from the steel-sheet #1, in which photo (a) is a low magnification view, and photo (b) is a high magnification view of the rectangular area in photo (a). Fig. 4 (c) and (d) are the EDX profiles at point E and point A respectively. The low magnification view (a) indicates that there are two regions on the surface of the steel-sheet #1, i.e., a region where particles are observed (particle region) and a region where no particle is observed (non-particle region). The high magnification view (b) covers both the regions. The EDX analysis of the point E in the non-particle region detected Si and O as shown in (c). In the profile, Cu has root in the sample holder of the TEM apparatus, while C is originated from the film of the extraction replica. The result indicates that the non-particle region consists of silicon oxide. The non-particle region has a more gray color tone. The color is consider to be caused by the oxide film of about 50 nm thick, as observed by the cross sectional TEM shown in Fig. 3. The non-particle region, or the region consisting of silicon oxide, was analyzed of its diffraction pattern. A diffraction spot, an indication of a crystalline structure, was not clearly observed as shown in Fig. 4 (c). Thus the silicon oxide is regarded as amorphous.

On the other hand, the EDX analysis of a spot in the particle region which is not covered by any particle (point A) exhibited no peak except for Cu from the TEM sample holder and C from the replica film as shown in Fig. 4 (d). The result indicates that no film-like oxide exists in the particle region. **Fig. 5** shows an observation result of a oxide particle. From the particle, Si and Mn were detected. Diffraction spot analysis revealed that the particular oxide is Mn_2SiO_4. From the above analyses, the surface of a steel-sheet having relatively high Si content, such as the steel-sheet #1, is considered to be unevenly covered by silicon oxide (Si_xO_y) as schematically illustrated in **Fig. 6**. Because this silicon oxide works as a barrier against the reaction of phosphate-treatment, the high Si concentration region is considered to prevent the formation of zinc phosphate crystal and thus affect the phosphatability significantly.

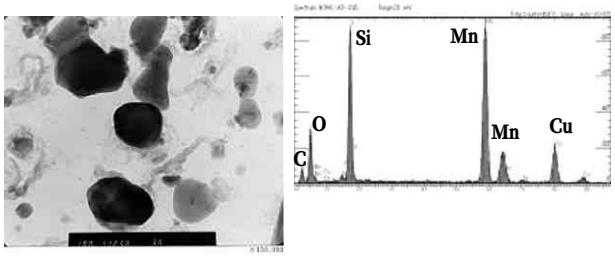

Fig. 5 Analysis of particles

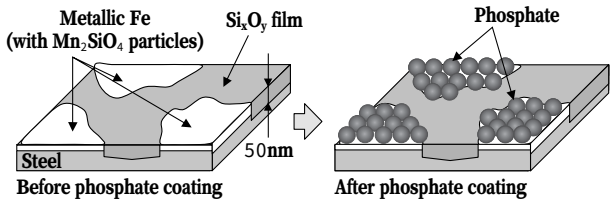

Fig. 6 Schematic structure of steel surface with high Si content

2.2 The types of surface oxides and their relation with phosphatability

Steel-sheet samples having different compositions were prepared to clarify the relation between the surface oxides and phosphatability. The samples were subjected to XPS analysis for the identification of oxide. Phosphatability of the samples were evaluated in relation to the oxides. **Fig. 7** shows the phosphatability of samples having different Si and Mn content. The symbols in the figure represent phosphatability in terms of "good" to "poor". The solid line in the figure represents the border for the formation of oxide. The concentration range below the line yields no silicon oxide and was found to exhibit good phosphatability. On the other hand, the concentration range above the line in Fig. 7 exhibits only poor phosphatability. This poor phosphatability is attributable to the silicon oxides formed on the steel-sheet surface. As described previously, in the region on the steel-sheet surface in which localized silicon oxide exist, the oxide works as a barrier against the crystal formation of zinc phosphate. In other word, good phosphatability of a steel-sheet is achieved by making the alloying elements reside below this line.

As has been known, Si is an effective element for improving mechanical properties of steel, since the element increases strength with minimum loss of elongation. Increasing Si content, however, may promote the formation of oxide and deteriorate phosphatability as shown in Fig. 7. This issue may possibly be avoided by simultaneously increasing Mn content, since the critical point of silicon oxide formation lies along a straight line of Si against Mn concentration as depicted in Fig. 7. In other words, by adjusting both the Si and Mn concentrations to optimum combinations, mechanical properties phosphatability can simultaneously be achieved, although these two has conventionally been regarded as trade-off.

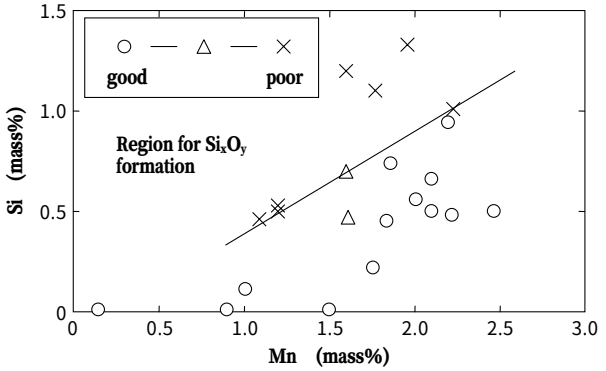

Fig. 7 Relationship between phosphatability and chemical composition

2.3 Trial production of steel-sheets having excellent phosphatability

Prototype high-strength, high-elongation steel-sheets having excellent phosphatability were prepared based on the above principle regarding alloying elements governing the surface oxides and phosphatability. Table 2 shows the compositions of the prototype steel-sheets. Both of the steel A and B are alloyed with relatively high concentrations of Si in order to achieve high strengths and elongations. Adequate amounts of Mn were added to the steel-sheets, based on the relation depicted in Fig. 7, so as to realize good phosphatability by preventing the formation of silicon oxide at these relatively high Si concentrations. The Mo content in steel A is added to further increase to the steel's strength to 980 MPa grade.

The steel-sheets of A and B were subjected to phosphate-treatment. The treated sheets A and B were confirmed to have sufficient amounts of zinc phosphate, 2.3 g/m^2 and 2.1 g/m^2 respectively. **Fig. 8** shows the surface appearances of the steel-sheets A and B after the treatment, indicating good phosphatability of both the steels. Also included in the figure are AES mappings of the steel-sheets before the treatment. No Si concentrated region was observed to be caused by silicon oxides. The coated sheets were also subjected to adhesion tests. **Fig. 9**

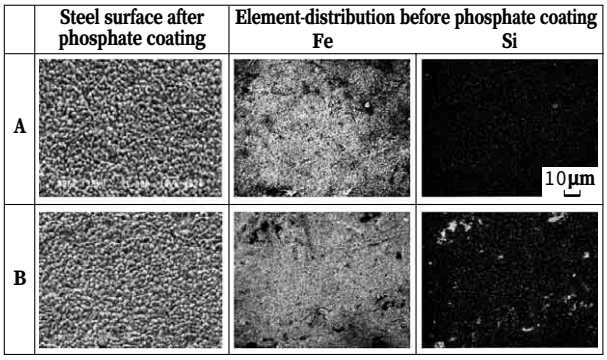

Fig. 8 Surface SEM micrographs after phosphate coating, and surface element-distribution before phosphate coating

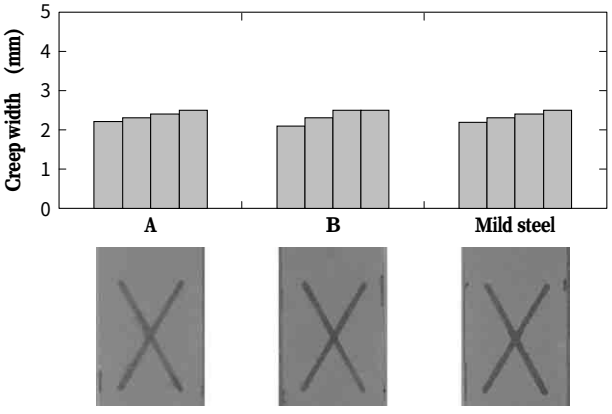

Fig. 9 Adhesion of paint film

Table 3 Mechanical properties of trial steels

Steel	YS (MPa)	TS (MPa)	El. (%)	YR (%)
A	701	1,003	15	70
B	720	1,027	16	70

depicts the creep widths of the paint films coated on the prototype steels and a mild steel. The appearances of the pieces after the tests are also shown in the figure. Mild steels are generally known to show good adhesion with paint film. Both the prototype steels exhibit adhesion characteristics comparable to that of mild steel. Thus, the prototype steels are confirmed to have good adhesion characteristics. The above result verifies that the oxide formations on the prototype steel-sheets are controlled in the intended manner. The formation of Silicon oxide is effectively prevented, which otherwise can adversely affects phosphatability, resulting in a good adhesion of paint films.

Table 3 summarizes the mechanical properties of the prototype steels. The steels have strengths falling in 980 MPa grade with elongations of about 15 %. Conventionally, addition of Si was restricted by its adverse effect on phosphatability[10), 11)], regardless of the fact that the addition of Si has been known to be effective in improving strength and elongation. The prototype steels, however, exhibit good phosphatability along with their high strengths and elongations. Such combination of properties is considered to be the result of adequately adding Mn to the high Si steels and thus preventing the formation of silicon oxides harmful to phosphatability.

Conclusions

The effect of surface oxide on phosphatability was analyzed. Based on the result of the analysis, prototype cold roll steel-sheet was prepared, which exhibits both good phosphatability and high mechanical strength. The following summarizes the results.

1) A region with concentrated Si may appear on a steel-sheet surface depending on the steel composition. The region consists of film-like silicon oxide formed on the steel-sheet surface. The film works as a barrier against the formation of zinc phosphate, a reaction product of phosphate-treatment.
2) The formation of the silicon oxide is affected by the Si and Mn content of steel and can effectively be prevented by adequately combining both the Si and Mn concentrations. A good phosphatability can be obtained for the steel having a high concentration of Si which is added to obtain good mechanical properties.
3) Prototype steel-sheets were prepared with additions of Si and Mn. Good phosphatability and mechanical properties are simultaneously achieved in a steel by adequately adding both the elements according to the result obtained in this study.

References

1) I. Tamura et al.: *Tetsu-to-Hagane*, Vol.59, No3 (1973) , p.454.
2) Y. Tomota et al.: *Tetsu-to-Hagane*, Vol.61, No.1 (1975) ,p.107.
3) Y. Omiya et al.: *R&D Kobe Steel Engineering Reports*, Vol.52, No.3 (2002) ,p.10.
4) T. Kashima et al.: *R&D Kobe Steel Engineering Reports*, Vol.52, No.3 (2002) ,p.15.
5) Y. Tsuchiya et al.: *Tetsu-to-Hagane*, Vol.86, No6 (2000) , p.396.
6) Y. Hirose et al.: *Tetsu-to-Hagane*, Vol.68, No6 (1982) , p.665.
7) M. Fukumoto et al.: *Tetsu-to-Hagane*, Vol.85, No12 (1999) , p.878.
8) T. Yamashita et al.: *CAMP-ISIJ*, 7 (1994) ,p.388.
9) C. Kato et al.: *CAMP-ISIJ*, 7 (1994) ,p.1511.
10) T. Hada et al.: *Journal of Surface Finishing Society of Japan*, Vol.41, No9 (1990) , p.927.
11) S. Maeda et al.: *Tetsu-to-Hagane,* Vol.68, No16 (1982) , p.2497.
12) M. Nomura et al.: *Tetsu-to-Hagane*, Vol.92, No6 (2006) , p.378.
13) S. Maeda et al.: *Boushoku-Gijutu*, Vol.25, No10 (1976) , p.597.